# Optimum Multiuser Modulation and Coding for Energy-Efficient Extended Reality (XR) Support

Sagnik Bhattacharya[1], Kamyar Rajabalifardi[1], Rohan Pote[2], Hyukjoon Kwon[2], Dongwoon Bai[2], John M. Cioffi[1]
[1]Dept. of Electrical Engineering, Stanford University, Stanford, CA, USA
[2]Samsung Semiconductors, San Diego, CA, USA
Emails: {sagnikb, kfardi, cioffi}@stanford.edu, {rohan.pote, hyukjoon.k, dongwoon.bai}@samsung.com

***Abstract*—In the ever-evolving landscape of Extended Reality (XR)-based distributed rendering, the scenario where the number of user antennas exceeds the number of access point (AP) antennas presents a low-rank channel problem. This often arising situation demands high data rates (upto 500 Mbps) and low power consumption. Current Wi-Fi solutions using OFDM-based power allocation fall short in addressing these requirements efficiently. This paper introduces a novel non-linear Generalized Decision Feedback Equalizer (GDFE) based algorithm to optimize the power allocation to elevate data rates and minimize energy usage, especially in low rank scenarios. Incorporating time-sharing techniques, the proposed algorithm offers substantial improvements over existing standards. Extensive experimental validations demonstrate that the proposed algorithm achieves 70% reduction in power consumption compared to OFDM-based current Wi-Fi standards, while maintaining the same data rates. Conversely, the proposed algorithm achieves 90% higher data rates compared to OFDM algorithm at the same SNR of 20 dB.**

***Index Terms*—extended reality (XR), augmented reality (AR), generalized decision feedback equalizer (GDFE), multiple access channel (MAC), time sharing**

## I. Introduction

This research explores distributed rendering in XR systems, emphasizing VR environments for collaborative experiences. It examines scenarios where users with VR headsets interact in a virtual space, sending visual data to a central server via Wi-Fi. The server processes and integrates these inputs into a unified 3D environment, then redistributes it to users, ensuring a seamless 360-degree view. This approach aims to enhance real-time immersion by leveraging high bandwidth, low latency, and low power wireless communication, crucial for effective and accessible XR applications. The uplink distributed rendering scenario is a multiple-input-multiple-output (MIMO) multiple-access channel (MAC). The multiple-access channel is a fundamental model in communication, characterizing a situation where multiple transmitters are sending information to a single receiver [1]. The uplink MIMO system with additive white gaussian noise (AWGN) can be expressed as:

$$\boldsymbol{y} = H \cdot \boldsymbol{x} + \boldsymbol{n} \tag{1}$$

Where $\boldsymbol{n}$ is the Gaussian noise, and $\boldsymbol{x}$, $\boldsymbol{y}$ are the transmitted and received signals, respectively.

Two primary challenges emerge as significant roadblocks for distributed XR rendering: the uplink bandwidth constraint and the edge devices' considerable power consumption, which have inherent resource constraints. XR heavily relies on Head-Mounted Displays (HMDs), which necessitate stringent adherence to power and weight limitations. The imperative to optimize the Quality-of-Experience (QoE) mandates that HMDs be lightweight and compact. Consequently, this necessitates the offloading of substantial computing and storage tasks to external processing units, such as computers or cloud-based servers. Complex three-dimensional imagery transmission, a cornerstone of these VR applications, necessitates data rates reaching upwards of 500 Mbps or more per user. However, existing wireless methods' capabilities, even those conforming to the latest Wi-Fi standards (802.11b/g/n/ac/be) [2], are insufficient for such high data rate demands, especially when the number of users' antennas exceeds the number of access-point (AP) antennas, and/or the channel is low rank. This issue complicates transmitting uplink 3D image data. Additionally, the current achievable data rates through Wi-Fi, while substantial, lead to prohibitive power consumption levels. This scenario is particularly challenging for devices like Augmented Reality (AR) glasses, where limited power resources are a critical constraint. These limitations significantly impede XR systems' development and practical realization suggest improved real-time data transmission for distributed VR rendering.

This work addresses these challenges by optimizing the data rates and the power consumption using a non-linear generalized decision feedback equalizer (GDFE) [1]. These systems achieve the maximum possible data rates for each of the $N$ users in a VR setting, considering factors such as the channel impulse responses between the users and the AP, the number of antennas, the distance from the AP, and the transmit signal-to-noise ratio at each user's device. In a converse approach, given each user's prerequisite minimum data rates, the objective minimizes the edge devices' power consumption. Tthe proposed GDFE-based solutions achieve much higher data rates with much lower power consumption, compared to current Wi-Fi standards, using the time-sharing (vertex sharing) technique. This dual optimization strategy also overcomes the prevailing bottlenecks in uplink communication capacity, thereby paving the way for high-fidelity XR systems' development and deployment.

A presented series of extensive experiments evaluate the proposed system's performance for Extended Reality (XR) applications. These experiments encompass a broad parameter range, which includes channel impulse responses, the number

of users involved, the quantity of antennas per user, requisite minimum data rates, signal-to-noise ratio (SNR), and the spatial distances from the access point (AP). The proposed GDFE-based approach augments the traditional Orthogonal Frequency Division Multiplexing (OFDM)-based Wi-Fi methods.

These GDFE results demonstrate a significant achievable-rate increase, reaching upwards of 500 Mbps per user antenna. This figure notably surpasses the data rates feasible through traditional Wi-Fi methodologies. Furthermore, results find a substantial energy-saving improvement. Specifically, for a given minimum required data rate, a threshold that traditional Wi-Fi can accomplish, the proposed algorithm achieves this benchmark with an order of magnitude lower user-device energy consumption. This finding is particularly impactful, considering the constraints of power resources in edge devices such as Augmented Reality (AR) glasses, commonly employed in XR systems.

## II. Related Work

Recent studies [3]–[6] underscore the critical need for low-power uplink wireless communication systems capable of supporting advanced extended reality (XR) applications' high data rates. Traditional approaches, such as orthogonal multiple access (OMA)-based techniques, have been extensively explored in this context. These techniques, including time division multiple access (TDMA) and orthogonal frequency division multiple access (OFDMA) [7], involve users transmitting either at distinct time intervals or using frequency-domain resource blocks. Although OMA methods' implementations are straightforward and efficient, they do not meet the high data rate demands, particularly uplink 500+ Mpbs requirements that surpass current Wi-Fi standards [2].

This limitation has sparked significant research interest in non-orthogonal multiple-access (NOMA) methods as a wireless-transmission alternative. The literature [8]–[12] extensively discusses these approaches and emphasizes power-domain NOMA with the AP's superposition coding (SC) use downlink and successive interference cancellation (SIC) based decoding uplink. This method demonstrates a considerable data-rate improvement for a given signal-to-noise ratio (SNR). However, even with these advancements, the data achieved rates represented as 3 bits/s/Hz and translating to 240 Mbps for an 80 MHz channel still do not meet high-quality XR applications' necessary thresholds [8]–[11]. Additionally, [12] simultaneously transmits and receives reflecting intelligent surfaces (STAR-RISs) in conjunction with NOMA communications. This approach has shown potential in achieving spectral efficiency rates up to 11.2 bits/s/Hz. Despite these promising results, the practical implementation of RISs introduces additional complexities that the community continues to address.

## III. Methodology

The Generalized Decision-Feedback Equalizer (GDFE) resolves multiuser crosstalk issues. To achieve this, each user's data is detected based on all previously decoded users with each symbol [1], [13].

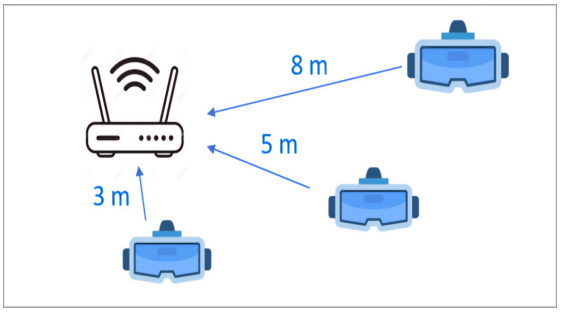


Fig. 1: XR Scenario

This work compares the performance of non-linear (GDFE) receivers [14] and linear receivers [15], both using basic OFDM. The specific focus is energy consumption. Initially, the receiver analysis uses the Simultaneous Water-Filling (SWF) algorithm [1] with the linear receiver. This SWF optimizes the sum data rate for a given available energy. Subsequently, a receiver uses the GDFE, targeting the data rate determined by the SWF algorithm, to minimize energy. The objective is to demonstrate how the GDFE receiver can substantially reduce energy consumption in attaining the same SWF data rate values obtained.

Notation includes: $U$ denotes the number of users. $\bar{N}$ represents the number of tones. $L_x$ and $L_y$ are the total number of users' antennas and the total number of antennas at the access point, respectively. $L_{x,u}$ is the number of antennas for the $u^{th}$ user. Moreover, the subscripts $u$ and $n$ represent user $u$ and $n^{th}$ tone, respectively. For instance, $H_u$ is user $u$'s channel matrix. There are two weighted-sum optimization problems: Energy Sum Minimization (III-A) and Data Rate Sum Maximization (III-B).

### A. Energy Sum Minimization

The weighted Energy Sum Minimization is formulated as follows:

$$\begin{aligned} \min_{\{R_{\boldsymbol{xx}}(u)\}} \quad & \sum_{u=1}^{U} w_u \cdot \operatorname{trace} \underbrace{\{R_{\boldsymbol{xx}}(u)\}}_{\mathcal{E}_u} \\ \text{s.t.} \quad & \mathbf{b} \succeq [b_{1,\min}, b_{2,\min}, \ldots, b_{U,\min}]^* \\ & \mathcal{E} \geq 0 \end{aligned} \tag{2}$$

Where $R_{\boldsymbol{xx}}(u)$ and $b_{u,\min}$ are the autocorrelation matrix and user $u$'s minimum data rate, respectively. Also, the vector $w \in \mathbb{R}^U_{0+}$ represents non-negative weights for each user's energy. The corresponding Lagrangian function is:

$$\begin{aligned} \mathcal{L}_{\min E}\left(R_{\boldsymbol{xx}}, \boldsymbol{b}, \boldsymbol{w}, \boldsymbol{\theta}\right) = \max_{\boldsymbol{\theta}} \min_{R_{\boldsymbol{xx}}} & \sum_{u=1}^{U} w_u \cdot \operatorname{trace}\{R_{\boldsymbol{xx}}(u)\} \\ & + \theta_u \cdot b_u - \theta_u \cdot b_{\min,u} \end{aligned} \tag{3}$$

*B. Data Rate Sum Maximization*

The weighted Data Rate Sum Maximization problem can be formulated as follows:

$$\begin{aligned} \max_{\{R_{\boldsymbol{xx}}(u)\}} \quad & \sum_{u=1}^{U} \theta_u \cdot b_u \\ \text{s.t.} \quad & \mathcal{E}_{\boldsymbol{x}} \preceq [\mathcal{E}_{1,\max}, \mathcal{E}_{2,\max}, \ldots, \mathcal{E}_{U,\max}]^* \\ & \mathbf{b} \succeq 0 \end{aligned} \tag{4}$$

Similar to the previous part, we can expand the Lagrangian function:

$$\begin{aligned} \mathcal{L}_{\max\, R}\left(R_{\boldsymbol{xx}}, \boldsymbol{b}, \boldsymbol{w}, \boldsymbol{\theta}\right) = \min_{\boldsymbol{w}} \max_{R_{\boldsymbol{xx}}} \sum_{u=1}^{U} w_u \cdot \operatorname{trace}\left\{R_{\boldsymbol{xx}}(u)\right\} \\ + \ \theta_u \cdot b_u - w_u \cdot \mathcal{E}_{\max,u} \end{aligned} \tag{5}$$

The common term $w_u \cdot \operatorname{trace}\{R_{\boldsymbol{xx}}(u)\} + \theta_u \cdot b_u$ in both optimization problems implies their duality. Therefore, a primal-dual approach solves the optimization problem.This locates the optimal autocorrelation matrix $R_{\boldsymbol{xx}}$, while fulfilling both the data rate and energy constraints.

It can be proven that the aforementioned optimization problems can be solved for each tone separately. In other words, an independent GDFE is assigned to each tone, and the total energy can be calculated by summing up all tones [1]. The corresponding energy minimization problem for each tone is as follows:

$$\begin{aligned} \min_{\{R_{\boldsymbol{xx}}(u,n)\}} \quad & \sum_{u=1}^{U} \sum_{n=0}^{\bar{N}} w_u \cdot \operatorname{trace}\left\{R_{\boldsymbol{xx}}(u,n)\right\} \\ \text{s.t.} \quad & \mathbf{b} = \sum_{n=0}^{\bar{N}} [b_{1,n}, b_{2,n}, \ldots, b_{U,n}]^* \succeq \boldsymbol{b}_{\min} \succeq \mathbf{0} \end{aligned} \tag{6}$$

Where $R_{\boldsymbol{xx}}(u,n) \in \mathbb{R}^{L_{x,u} \times L_{x,u}}$ is the autocorrelation matrix of $\boldsymbol{x}$ for user $u$ on the $n^{th}$ tone.

Similarly, the data rate maximization problem per each tone is:

$$\begin{aligned} \max_{\{R_{\boldsymbol{xx}}(u,n)\}} \quad & \sum_{u=1}^{U} \theta_u \cdot \left\{ \sum_{n=0}^{\bar{N}} b_{u,n} \right\} \\ \text{s.t.} \quad & \mathcal{E} = \sum_{n=0}^{\bar{N}} [\mathcal{E}_{1,n}, \mathcal{E}_{2,n}, \ldots, \mathcal{E}_{U,n}]^* \preceq \boldsymbol{\mathcal{E}}_{\max} \ . \end{aligned} \tag{7}$$

Equation 6 's Lagrangian function is:

$$\begin{aligned} \mathcal{L}_{\min\, E}\left(R_{\boldsymbol{xx}}, \boldsymbol{b}, \boldsymbol{w}, \boldsymbol{\theta}\right) = \left( \sum_{u=1}^{U} \theta_u \cdot b_u \right) + \\ \sum_{n=0}^{\bar{N}-1} \underbrace{\{ \sum_{u=1}^{U} [w_u \cdot \operatorname{trace}\left\{R_{\boldsymbol{xx}}(u,n)\right\} - \theta_u \cdot b_{u,n}]\}}_{\mathcal{L}_n\left(R_{\boldsymbol{xx}}(n), \boldsymbol{b}_n, \boldsymbol{w}, \boldsymbol{\theta}\right)} \end{aligned} \tag{8}$$

Where $R_{\boldsymbol{xx}}(n) = \operatorname{blkdiag}\{R_{\boldsymbol{xx}}(U,n), \ldots, R_{\boldsymbol{xx}}(1,n)\}$, and the operator blkdiag aligns matrices along the diagonal of another matrix. The term $\mathcal{L}_n\left(R_{\boldsymbol{xx}}(n), \boldsymbol{b}_n, \boldsymbol{w}, \boldsymbol{\theta}\right)$ is called the Tonal Lagrangian term. Since $\mathcal{L}_n$ does not depend on $b_u$, minimizing the tonal lagrangian term is synonymous with optimizing:

$$\mathcal{L}_{\min\, E}(\boldsymbol{\theta}, n) \triangleq \min_{\{R_{\boldsymbol{xx}}(u,n), b_{u,n}\}} \mathcal{L}\left(R_{\boldsymbol{xx}}(n), \boldsymbol{b}_n, \boldsymbol{w}, \boldsymbol{\theta}\right) \tag{9}$$

Therefore, the min-max problem 8 reduces to :

$$\mathcal{L}^*_{\min\, E} = \max_{\boldsymbol{\theta}} \{ \left[ \sum_{n=0}^{\bar{N}-1} \mathcal{L}_{\min\, E}(\boldsymbol{\theta}, n) \right] + \underbrace{\sum_{u=1}^{U} \theta_u \cdot b_u}_{\text{independent of } R_{\boldsymbol{xx}}(u,n), n} \ \} \tag{10}$$

Moreover, the data rates must lie in the system's capacity region. The capacity region, denoted as $\mathcal{C}(b)$, refers to the set of all possible rate vectors $b$ for users with independent messages, where each message employs a code that achieves the single-user capacity. This code is used for all systems and differences in their performance therefore solely derives from the GDFE improvement over the linear receiver. This set characterizes the rates at which all users can be reliably decoded with a negligible average error probability by a Maximum A Posteriori (MAP) detector or equivalently, a Maximum Likelihood (ML) detector with equally likely messages for all independent users. The capacity region is essentially the combination of rates at which the system can operate such that all users' messages are delivered correctly. The capacity region follows from the Shannon capacity formula as [16]:

$$0 \leq b_n \leq \log_2 \left| \left( \sum_{u=1}^{U} \widetilde{H}_{u,n} \cdot R_{\boldsymbol{xx}}(u,n) \cdot \widetilde{H}^*_{u,n} \right) + I \right| \tag{11}$$

$\tilde{H}_{u,n} = R_{NN}^{-1/2}(n) \cdot H_{u,n}$ is the equivalent-white-noise channel per each tone.

A semi-definite programming (SDP) method solves the inner part of the optimization problem 10 ($\mathcal{L}_{\min\, E}(\boldsymbol{\theta}, n)$), while an Ellipsoid method [17]

If the channel matrix $H_{u,n}$ is non-singular with the ideal common codes mentioned ($\Gamma = 0$dB), the ellipsoid method finds a unique optimal solution. In other words, the system assigns different dimensions, such as time and frequency, to each user separately. However, if the channel is singular, the Hessian matrix computed at each ellipsoid-method iteration degradeds, and the optimization problem does not have a unique solution. In this case, the algorithm allows more than one user to use some specific dimensions at the same time, which is known as "time-sharing". When the users "time-share" with one another, the algorithm only finds the weighted sum. A separate time-sharing step then applies to ensure all users meet their target data rate.

This minPMAC algorithm appears as Algorithm 2. Initially, the SWF algorithm provides first ellipsoid parameters. Then, minPMAC alternates between two optimization problems until convergence. It prioritizes the users' decoding process based on $\theta$ at each iteration.

**Algorithm 1** SWF

**Inputs:** $H, L_x, R_{nn}$

**for** $u = 1, 2, \ldots, U$ **do**

$R_{\text{noise}}(u) \triangleq \sum_{i \neq u} H_i \cdot R_{\boldsymbol{xx}}(i) \cdot H_i^* + R_{\boldsymbol{nn}}$

$R_{\text{noise}}^{-1/2}(u) \cdot H_u = F_u \cdot \Lambda_u \cdot M_u^*$

**for** $\ell = 1, 2, \ldots, L_x$ **do**

$\mathcal{E}_{u,\ell} = \max\left\{0, \frac{1}{L_x}\left(\mathcal{E}_u - \sum_{k=1}^{L_x} \frac{1}{\lambda_{u,k}^2}\right) - \frac{1}{\lambda_{u,\ell}^2}\right\}$

**end for**

**end for**

**return** $\mathcal{E}_u$

**Algorithm 2** minPMAC

**Inputs:** $H$, $L_{xu}$, $b_u$, $w$

**Initialize:** $A$, $\theta$ using SWF

**while** the sum rate doesn't converge **do**

$\pi \triangleq$ Indices of sorted $\theta$ in descending order

**for** $n = 1, 2, \ldots, \bar{N}$ **do**

**for** $u = 1, 2, \ldots, U$ **do**

$\mathcal{E}_{u,n} = \text{trace}\left(R_{\boldsymbol{xx}}\left(\pi^{-1}(u), n\right)\right)$

$\mathcal{R}_{u,n} \triangleq \log_2 \left|\sum_{i=u}^{U} \tilde{H}_{\pi^{-1}(i),n} \cdot R_{\boldsymbol{xx}}\left(\pi^{-1}(i), n\right) \cdot \tilde{H}_{\pi^{-1}(i),n}^* + I\right|$

**end for**

$$b_{u,n}^* = \underset{R_{\boldsymbol{xx}}}{\text{argmin}} \quad \sum_{u=1}^{U} w_u \cdot \mathcal{E}_{u,n} - \left(\theta_{\pi^{-1}(u)} - \theta_{\pi^{-1}(u+1)}\right) \cdot \mathcal{R}_{u,n}$$

$$\text{s.t.} \quad R_{\boldsymbol{xx}} \succeq \mathbf{0}$$

**end for**

$g = \sum_{n=1}^{\bar{N}} b_{u,n}^* - b_u$

$\tilde{g} = \frac{1}{\sqrt{g^T A g}} g$

$\theta = \theta - \frac{1}{U+1} \frac{Ag}{\sqrt{g^T A g}}$

$A = \frac{U^2}{U^2-1}\left(A - \frac{2}{U+1} A \tilde{g} \tilde{g}^T A\right)$

**return** $b_{u,n}^*$, $\mathcal{E}_{u,n}$

## IV. Performance Evaluation

In our experimental setup, we simulate a virtual reality (VR) gaming environment involving $N$ users, each engaging in a distributed rendering task. These users, equipped with VR glasses, receive fragmented visual perspectives of a virtual room. We define $L_{xu}$ as a 1x$N$ array, representing the number of antennas at each user's device. Additionally, the access point (AP) is equipped with $L_y$ antennas. The spatial positioning of users relative to the AP is modeled through a uniform random distribution, with distances ranging between $d_{\text{min}}$ and $d_{\text{max}}$. For the characterization of channel impulse responses between user devices and the AP, we utilize a dataset of over 10,000 channel realizations provided by Samsung. These realizations are based on WiFi 802.11ax standards [18], specifically tailored for model B (indoor residential) and model D (indoor office) scenarios. At any given moment, our experimental framework randomly selects one of these channel impulse responses for each pairing of the user device antenna and AP antenna. We multiply an additional components for path loss and shadow fading. We use the following combination of path loss and shadow fading loss:

$$\begin{aligned} L(d) &= L_{path}(d) + L_{shadow}(d) \quad \text{dB} \qquad d \leq d_{break} \\ &= L_{path}(d_{break}) + L_{shadow}(d_{break}) + \\ &\qquad 35 \log_{10}\left(\frac{d}{d_{break}}\right) \quad \text{dB} \qquad d > d_{break} \end{aligned} \tag{12}$$

where the break-point distance is $d_{break} = 5\, m$, and

$$L_{path} = 20 \log_{10}(f) + 20 \log_{10}(d) - 147.5\text{dB} \tag{13}$$

and $L_{shadow}$ is a random log-normal variable sampled from $\frac{1}{\sqrt{2\pi\sigma_z^2}} \exp -(L_{shadow}(d)^2/(2\sigma_z^2))$, $\sigma_z$ is 3dB before break-point distance and $4dB$ after the breakpoint. The channel delay taps are spaced 10 ns apart, hence the channel bandwidth is 100 MHz. In our experiments,we use the center frequency $f_c = 5GHz$ and vary the Fast Fourier Transform length ($fft_{length}$). Fig. 2 shows an instance of the channel impulse responses used in the experiments. The parameters used for the experiments are tabulated in Table I. We vary the transmit Signal-to-Noise Ratio (SNR) values and assess the resultant data rates achieved by both the baseline OFDM-based system and our proposed GDFE-based algorithm. Conversely, by setting variable minimum required data rates, we evaluate and compare the power consumption metrics for both the proposed algorithm and the baseline system. The ranges over which each of these parameters is varied are systematically tabulated for clarity and ease of reference.

TABLE I: Experiment Parameters

| Parameter | Value |
|---|---|
| Number of users $N$ | {2, 3} |
| Number of antennas per user $L_{xu}$ | 1 |
| Number of antennas at AP $L_y$ | {2, 3, 4} |
| User to AP distance range $[d_{min}, d_{max}]$ | [1m, 10m] |
| Channel bandwidth $W$ | 100 MHz |
| Number of channel delay taps $n_{delay}$ | {9, 18} |
| FFT length $fft_{length}$ | {16, 32, 64, 128, 256} |
| SNR | [-10, 50] dB |

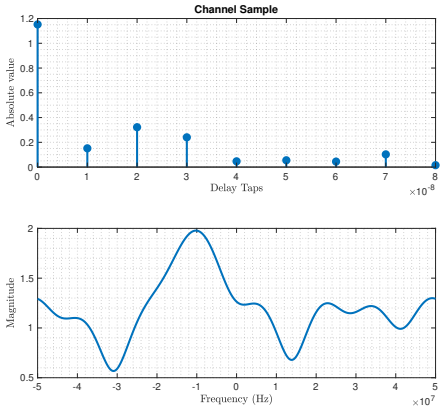


Fig. 2: Channel B Samples

TABLE II: Parameters for 2 Experiment Scenarios

| Parameter | Case 1 | Case 2 |
|---|---|---|
| **Antennas/user** | 1 | 1 |
| **AP Antennas** | 2 | 2 |
| **Users** | 2 | 3 |
| **Distance from AP (m)** | {3, 3} | {3, 3, 3} |
| **Data Rates (OFDM) (Mbps)** | {239, 481} | {136, 236, 266} |
| **Data Rates (Proposed) (Mbps)** | {239, 481} | {470, 470, 470} |
| **Energy (OFDM)** | {1, 1} | {1, 1, 1} |
| **Energy (Proposed)** | {0.1168, 0.2870} | {0.3437, 0.9621, 0.9308} |

TABLE III: Energy Consumption versus Number of AP Antennas for Single Antenna Per User, $R = 201.702$ Mbps, $U = 3$, $L_{xu} = 1$, distance from AP $= \{3m, 3m, 3m\}$

| AP Antennas | OFDM | | Proposed Algorithm | |
|---|---|---|---|---|
| | **Energy** | **Energy$_{avg}$** | **Energy** | **Energy$_{avg}$** |
| 1 | [1, 1, 1] | 1 | [0.5721, 0.5417, 1.1325] | 0.7488 |
| 2 | [0.9, 0.9, 0.9] | 0.9 | [0.1354, 0.0422, 0.1552] | 0.1109 |
| 3 | [0.75, 0.75, 0.75] | 0.75 | [0.0294, 0.0750, 0.0893] | 0.0646 |
| 4 | [0.3, 0.3, 0.3] | 0.3 | [0.0214, 0.0508, 0.0556] | 0.0426 |

Table II shows 2 instances of the experiment results using varying parameters. As we see from the first column, for the same data rates, the proposed algorithm consumes an order of magnitude less relative energy as compared to OFDM baselines. This shows that, even in the case where the total number of antennas at all users (2) is equal to the total number of antennas at the AP (2), harsh channel conditions and crosstalk between the subchannels lead to significant energy savings compared to OFDM, when using the proposed non-linear feedback-based algorithm. The second column stresses the channel further, i.e. forces it into a low-rank situation where the total number of antennas at the users (3) is less than the total number of antennas at the AP (2). Row lank regimes are where we see the massive benefit of using GDFE-based power allocation. This is aided by time sharing between users and thus simultaneous power allocation in the same time and frequency slot, which OFDM is incapable of. We achieve, on an average, 2 times the data rate at half the energy requirement.

Table III demonstrates the proposed algorithm's superiority over the baseline OFDM in power efficiency across various AP antenna counts, maintaining a fixed data rate of 200 Mbps/user. The proposed algorithm using GDFE achieves the same data rates with 72.5% lower power consumption on an average. The power savings become more pronounced as AP antennas decrease, attributed to the channel's lower rank in these scenarios, highlighting the algorithm's effectiveness in energy conservation under channel constrains. For the last row, where the number of antennas at AP (4) exceeds the number of user antennas (3), we see that the GDFE-based algorithm takes advantage of the crosstalk in the channel and achieves the required data rates at significantly lower energy compared to OFDM. Table IV demonstrates the the energies required by the GDFE-based proposed algorithm to achieve the same data rates as achieved by the current Wi-Fi linear OFDM algorithm, with increasing number of AP antennas. For this figure, we keep the energy used by the OFDM based algorithm to be a constant, and compute the energies required by the proposed algorithm to achieve the corresponding data rates. We see that the proposed algorithm achieves, on an average, 70.7% lower power consumption in this case, compared to OFDM method.

TABLE IV: Energy Consumption versus Number of AP Antennas for Single Antenna Per User, Fixed energy for OFDM, $U = 3$, $L_{xu} = 1$, distance from AP $= \{3m, 3m, 3m\}$

| AP Antennas | OFDM | | Proposed Algorithm | |
|---|---|---|---|---|
| | **Energy** | **Data Rates** | **Energy** | **Data Rates** |
| 1 | [1, 1, 1] | [204, 174, 175] | [1.1534, 0.5194, 0.7641] | [204, 174, 175] |
| 2 | [1, 1, 1] | [224, 87, 210] | [0.0259, 0.1662, 0.1737] | [87, 164, 270] |
| 3 | [1, 1, 1] | [233, 117, 200] | [0.0233, 0.1171, 0.1223] | [18, 210, 322] |
| 4 | [1, 1, 1] | [290, 180, 252] | [0.1818, 0.1738, 0.0938] | [408, 202, 112] |

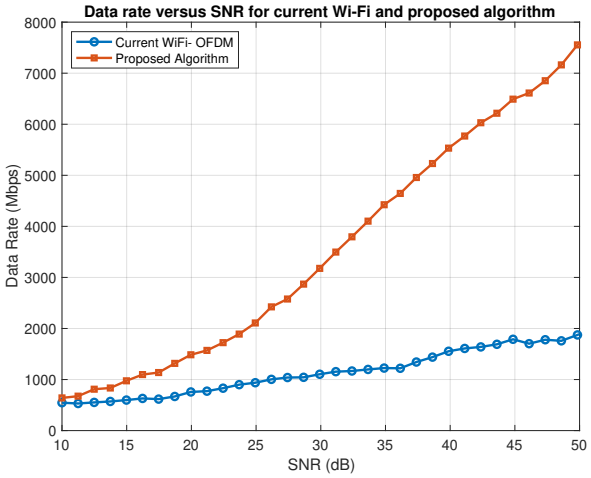


Fig. 3: Sum Rate versus SNR for Single Antenna Per User: Current Wi-Fi OFDM and Proposed Algorithm

Fig. 3 shows the sum rate across 3 users located at equal distances of 3 m from the AP, as a function of SNR (dB). We see that the slope of increase of the data rates for the proposed algorithm is significantly higher than that for the OFDM-based current Wi-Fi algorithm. Specifically, at an SNR of 20 dB, the propsed algorithm achieves a sum rate of 1500 Mbps across 3 users, as compared to the OFDM-based linear algorithm which

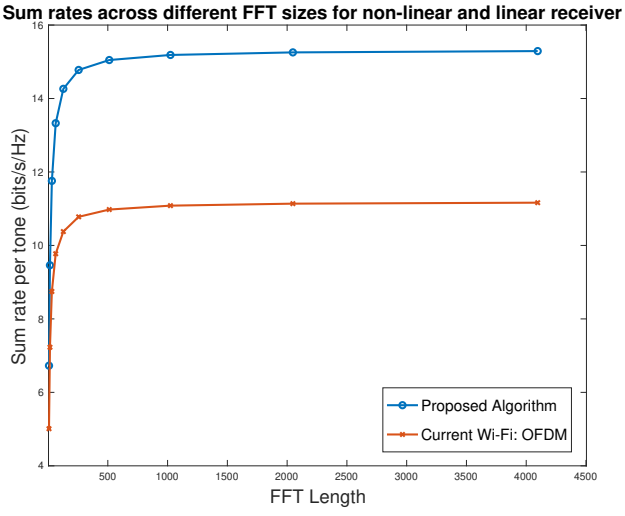


Fig. 4: Sum rate versus FFT length for equidistant users with single antenna per user

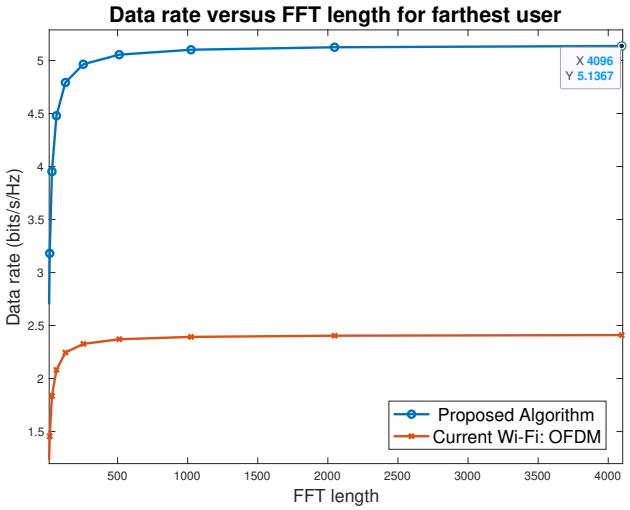


Fig. 5: Data rate versus FFT length for the farthest user with user distances from AP = {3m, 5m, 8m}, and single antenna per user

achieves 800 Mbps. The inability of the OFDM-based system to utilize crosstalk between the channels is evident, and this crosstalk is utilized by the proposed algorithm to achieve high data rates, especially at high SNR values. There is time sharing between the three users. The first user has to suffer in data rates by treating the other two user's signals as noise, and the second user does this for the third user's signal. However, the third user gets to fully exploit all the available dimensions, which contributes to the high data rates.

Fig. 4 and Fig. 5 compare the spectral efficiencies of a proposed algorithm against current Wi-Fi OFDM in equidistant users (3m, 3m, 3m) and non-equidistant users (3m, 5m, 8m) scenarios. As per Fig. 4, the proposed algorithm achieves 15 bits/s/Hz sum rates (500 Mbps/user) with FFT lengths 1024, outperforming OFDM's 11 bits/s/Hz. In Fig. 5, i.e., in non-equidistant setups, it ensures even the farthest user achieves equal data rates despite higher path losses, leveraging GDFE-based noise cancellation and time-sharing. The OFDM algorithm, which uses the water-filling algorithm for power allocation, fails to achieve this and hence the farthest user has the worst data rates of 2.3 bits/s/Hz at saturation. This demonstrates the proposed solution's superiority in energy and data rate efficiency, especially in low-rank channel conditions, making it a promising alternative to current Wi-Fi standards.

## V. Conclusion and Future Work

In this paper, we propose a novel Generalized Decision Feedback Equalizer (GDFE) strategy for power allocation that significantly enhances data rates and energy efficiency in low-rank channel conditions, which are particularly challenging for Extended Reality (XR) applications. Our comprehensive performance evaluation demonstrates that this approach markedly outperforms existing Wi-Fi methods, offering a promising solution for uplink communications in XR systems. Future directions include the integration of adaptive mechanisms and machine learning models to optimize power allocation dynamically, catering to real-time changes in channel conditions and further boosting the system's performance.

## References


[1] J. Cioffi, "Data transmission theory," vol. 40, no. 4, pp. 49–60, 2024. [Online]. Available: https://cioffi-group.stanford.edu/ee379a/course_reader.html

[2] *IEEE 802.11ax-2021 - IEEE Standard for Information Technology–Telecommunications and Information Exchange Between Systems Local and Metropolitan Area Networks–Specific Requirements - Part 11: Wireless LAN Medium Access Control (MAC) and Physical Layer (PHY) Specifications*, Institute of Electrical and Electronics Engineers, New York, NY, USA, 2021, iEEE 802.11ax-2021 (Wi-Fi 6/6E).

[3] I. F. Akyildiz and H. Guo, "Wireless communication research challenges for extended reality (XR)," *ITU Journal on Future abd Evolving Technologies*, vol. 3, 2022. [Online]. Available: https://www.itu.int/pub/S-JNL-VOL3.ISSUE2-2022-A24

[4] S. Shekhar, S. K. Feiner, and W. G. Aref, "Spatial computing," *Commun. ACM*, vol. 59, no. 1, p. 72–81, dec 2015. [Online]. Available: https://doi.org/10.1145/2756547

[5] Y. Siriwardhana, P. Porambage, M. Liyanage, and M. Ylianttila, "A survey on mobile augmented reality with 5g mobile edge computing: Architectures, applications, and technical aspects," *IEEE Communications Surveys Tutorials*, vol. 23, no. 2, pp. 1160–1192, 2021.

[6] T. Braud, F. H. Bijarbooneh, D. Chatzopoulos, and P. Hui, "Future networking challenges: The case of mobile augmented reality," in *2017 IEEE 37th International Conference on Distributed Computing Systems (ICDCS)*, 2017, pp. 1796–1807.

[7] M. Louie, D. Rouffet, and K. GILHOUSEN, "Multiple access techniques and spectrum utilization of the globalstar mobile satellite system," in *14th International Communication Satellite Systems Conference and Exhibit*, 1992, p. 1929.

[8] S. M. R. Islam, N. Avazov, O. A. Dobre, and K.-s. Kwak, "Power-domain non-orthogonal multiple access (noma) in 5g systems: Potentials and challenges," *IEEE Communications Surveys Tutorials*, vol. 19, no. 2, pp. 721–742, 2017.

[9] Y. Saito, Y. Kishiyama, A. Benjebbour, T. Nakamura, A. Li, and K. Higuchi, "Non-orthogonal multiple access (noma) for cellular future radio access," in *2013 IEEE 77th Vehicular Technology Conference (VTC Spring)*, 2013, pp. 1–5.

[10] A. Benjebbour, K. Saito, A. Li, Y. Kishiyama, and T. Nakamura, "Non-orthogonal multiple access (noma): Concept, performance evaluation and experimental trials," in *2015 International Conference on Wireless Networks and Mobile Communications (WINCOM)*, 2015, pp. 1–6.

[11] U. Ghafoor, M. Ali, H. Z. Khan, A. M. Siddiqui, and M. Naeem, "Noma and future 5g b5g wireless networks: A paradigm," *Journal of Network and Computer Applications*, vol. 204, p. 103413, 2022. [Online]. Available: https://www.sciencedirect.com/science/article/pii/S1084804522000728

[12] J. Zuo, Y. Liu, Z. Ding, L. Song, and H. V. Poor, "Joint design for simultaneously transmitting and reflecting (star) ris assisted noma systems," *IEEE Transactions on Wireless Communications*, vol. 22, no. 1, pp. 611–626, 2023.

[13] W. Yu and J. M. Cioffi, "Sum capacity of gaussian vector broadcast channels," *IEEE Transactions on information theory*, vol. 50, no. 9, pp. 1875–1892, 2004.

[14] J. M. Cioffi and G. Forney Jr, "Generalized decision-feedback equalization for packet transmission with isi and gaussian noise," pp. 79–127, 1997.

[15] R. W. Chang, "Synthesis of band-limited orthogonal signals for multichannel data transmission," *Bell system technical journal*, vol. 45, no. 10, pp. 1775–1796, 1966.

[16] C. E. Shannon, "A mathematical theory of communication," *The Bell System Technical Journal*, vol. 27, pp. 379–423, 1948. [Online]. Available: http://plan9.bell-labs.com/cm/ms/what/shannonday/shannon1948.pdf

[17] D. B. Yudin and A. S. Nemirovski, "Constrained minimization methods in the space of probability measures," 1976.

[18] "Ieee standard for information technology–telecommunications and information exchange between systems local and metropolitan area networks–specific requirements part 11: Wireless lan medium access control (mac) and physical layer (phy) specifications amendment 1: Enhancements for high-efficiency wlan," *IEEE Std 802.11ax-2021 (Amendment to IEEE Std 802.11-2020)*, pp. 1–767, 2021.